Heliyon

ELSEVIER

Received:
29 November 2018
Revised:
8 March 2019
Accepted:
15 March 2019

Cite as: Xiang Li, Pengfei Zhu, Lihong Han, Tao Zhang, Baonan Jia, Shanjun Li, Jun Chen, Ming Lei, Pengfei Lu. First-principles study of dehydration process of potassium dihydrogen phosphate crystal. Heliyon 5 (2019) e01384.
doi: 10.1016/j.heliyon.2019.e01384

First-principles study of dehydration process of potassium dihydrogen phosphate crystal

Xiang Li [a,b], Pengfei Zhu [a], Lihong Han [a], Tao Zhang [c], Baonan Jia [a], Shanjun Li [c,], Jun Chen [d], Ming Lei [b], Pengfei Lu [a,*]**

[a] *State Key Laboratory of Information Photonics and Optical Communications, Ministry of Education, Beijing University of Posts and Telecommunications, Beijing 100876, China*

[b] *School of Science, Beijing University of Posts and Telecommunications, Beijing 100876, China*

[c] *College of Electrical Engineering and Information Technology, Sichuan University, Chengdu 610065, China*

[d] *Beijing Applied Physics and Computational Mathematics, Beijing 100088, China*

[*] Corresponding author.

[**] Corresponding author.

E-mail addresses: lishanjun@scu.edu.cn (S. Li), photon.bupt@gamil.com (P. Lu).

Abstract

KDP crystal is showing a good property in high-power laser systems. However, working in a high-power environment is easy to have damaged-defect. Dehydration of KDP crystal is one of the damage phenomena. We explore the total energy and physical properties of the KDP crystal progressive dehydration by using First-principles calculations. It is found that the band gap of the KDP crystal gradually decreases with the deepening of dehydration, and there are many obvious defect states between 4 eV and 8 eV (the corresponding wavelength region is from 310 nm to 155 nm). It indicates that dehydration causes a reduction in the damage threshold of the KDP crystal. Our results indicate that these defect states are due to the change of hybridization type of P atoms, which is gradually transformed from original sp^3 hybridization to sp^2 hybridization in the dehydration process. An obvious redshift can be observed in the absorption spectrum, producing many distinct absorption peaks. All of the

https://doi.org/10.1016/j.heliyon.2019.e01384

results can provide the good basis for deeply understanding the electronic and optical properties of the KDP crystal.

Keywords: Materials science, Condensed matter physics

1. Introduction

KDP (Potassium Dihydrogen Phosphate, abbreviated as KH_2PO_4, KDP) crystal is a large-sized single crystal, which is widely used in high power laser systems [1]. It has many excellent features such as large nonlinear optical coefficients, high laser damage threshold, wide transmission band and easy phase matching. These advantages make KDP crystal widely applied in laser-inertia confinement fusion. Especially with the application of high-power laser systems in controlled thermonuclear reactions and the simulation of nuclear explosion, KDP crystal has attracted a lot of attention. However, the presence of defects in the KDP crystal greatly affects its application. For KDP crystal, non-uniform growth process may cause various defects [2, 3, 4, 5]. It is generally believed that laser-induced damage is associated with laser absorption of structural defects in KDP [9, 10]. In addition, KDP crystal is also susceptible to external factors such as high temperature, high pressure [6, 7, 8] and so on. Once the laser is irradiated for a long time, KDP is heated at high temperature, which may cause the dehydration [11, 12, 13].

There are many investigations on KDP at high temperature, such as phase change caused by high temperature, and conductivity variations induced by high temperature dehydration [14, 15]. In 2005, R.A. Negres *et al.* observed a new spectral feature during the laser-induced breakdown of KH_2PO_4 crystal. They attributed this to the dehydration product KPO_3 of KH_2PO_4 crystals. The product of thermal dehydration of KDP crystal is polymerized potassium metaphosphate $(KPO_3)_n$ [12], also known as Kurrol's salt C. It was proposed that dehydration was due to the thermally induced decomposition of KDP during laser-induced decomposition [16]. In 2009, R.A. Negres *et al.* evaluated KDP dehydration kinetics and thermodynamic parameters in the study of the crystal growth, thermal, optical and dielectric properties of L-lydine doped KDP crystal and L-alanine doped KDP [17, 18]. In 2010, P. Shenoy *et al.* used thermogravimetric analysis (TGA) and differential thermal analysis (DTA) to study the dehydration kinetics and high-temperature phase behavior [19]. In 2011, T. Tsujibayashi *et al.* observed that infrared laser-induced dehydration forms molecular chains in L-cysteine and potassium dihydrogen phosphate [20]. In 2013, C.E. Botez *et al.* explored that heating can cause dehydration of KDP and DKDP, which in turn led to structural changes [21]. In 2013, H. Ettoumi *et al.* studied the dehydration kinetics of KH_2PO_4 at the melting temperature and found that the heat treatment of KDP

https://doi.org/10.1016/j.heliyon.2019.e01384

at melting temperatures at different durations showed that the dehydration of KDP was gradual and the product was the mixture of KPO_3, $K_2H_2P_2O_7$ and $K_nH_2P_nO_{3n+1}$ [22]. Up to now, no further discussion has been conducted on the effects of the dehydration of KDP crystal on optical and electronic properties. The dehydration of KDP crystal is likely to produce some defects and optical absorption peaks due to these defects, which are likely to affect the application of KDP.

In this work, we built a 32-atom KDP crystal model and used First-principles method to optimize it to get a stable KDP crystal structure. We selected four sample models based on the KDP crystal model to simulate the dehydration process of KDP crystal and calculated their electronic and optical properties with Heyd-Scuseria-Ernzerhof (HSE) method [23, 24, 25, 26, 27]. Our calculations indicate that during the dehydration process of KDP, the bandgap value gradually decreases, and an obvious redshift can be observed in the absorption spectrum, resulting in many obvious optical absorption peaks and many defect states in the range of 4 eV to 8 eV. These defect states are mainly due to the change of P atoms from sp^3 hybridization to sp^2 hybridization. This structure reasonably explains the approximate process of dehydration of KDP crystal.

2. Materials & methods

First-principles simulations [28, 29, 30, 31] have been performed in the framework of Density-Functional theory (DFT) by using the plane wave-pseudopotential code VASP (Vienna *ab initio* simulation package) [32, 33]. The unit cell parameters are $a = b = c = 7.5021$ nm. A supercell of 32 atoms is built for the simulation of dehydration process [34, 35]. Cutoff energy was chosen highly enough as 350 eV to ensure the convergence of the electron wave function expanded in plane waves. The optimization will be accomplished by following the condition that a relatively high accuracy for the ground state electronic convergence limit is at 10^{-4} eV and force convergence is at 0.01 eV/Å. General gradient approximation (GGA) with Perdew-Burke-Ernzerhof (PBE) was adopted to describe the electron correlation [36, 37]. Previous researchers used the PBE method when studying the electronic properties of KDP [5, 38, 39]. We used the Heyd-Scuseria-Ernzerhof (HSE) [23, 24, 25, 26, 27] method to calculate the electronic properties and optical properties, because the band gap value obtained by HSE is 7.1 eV, which is closer to the experimental value than the 5.9 eV of PBE (the experimental value of the band gap is 7.2 eV) [2, 3, 4, 5, 40]. Our work solves the problem that the theoretical result for the KDP bandgap in the past is much smaller than the experimental result, making the calculation result more accurate and credible. The polyhedral structure model of pure KDP crystal is shown in Fig. 1.

https://doi.org/10.1016/j.heliyon.2019.e01384

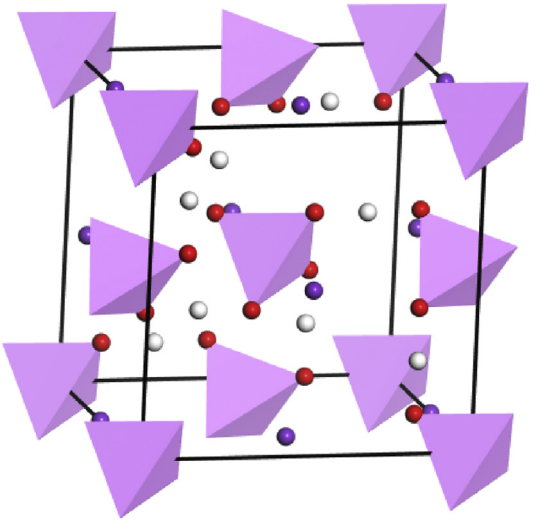

Fig. 1. The polyhedral structure model of pure KDP crystal.

3. Results & discussion

3.1. Structure and formation energy

Dehydration of KDP is a continuous process with increasing temperature. According to Ref. [41], the KDP dehydration process is divided into three stages. In the first stage, the $P_2O_7^{2-}$ group appears, meaning that the decomposition of the first stage KDP crystal proceeds in the direction of $K_4P_2O_7$. In the second stage, the intermediate phase product produced by the first stage continues to decompose. In the third stage, the products of the first two stages continue to decompose and reach the final state of decomposition. As a result, KDP is completely dehydrated and decomposed into polymer $(KPO_3)_n$. Similar analysis is also mentioned in Ref. [42]. The specific process of KDP dehydration can be expressed by formula (1) and formula (2) [43, 44]. Formula (1) shows the intermediate process of dehydration of KDP. Formula (2) expresses the final state of KDP dehydration, and the polymer $(KPO_3)_n$ is its final product.

$$nKH_2PO_4 \rightarrow K_nH_2P_nO_{3n+1} + (n-1)H_2O, n \geq 1 \quad (1)$$

$$K_nH_2P_nO_{3n+1}, n \gg 1 \cong (KPO_3)_n \quad (2)$$

In this process, we have selected four states as samples for analysis. According to formula (1), the first three models of dehydration were established by removing one molecule, representing the intermediate process. The last model removed all the water molecules in the KDP and simulated the final dehydration state in the final step represented by (2). The corresponding four dehydration models are shown in Fig. 2. In this way, for each water molecule removed, a model is chosen as an intermediate sample for analysis, which makes it more meaningful to compare the

https://doi.org/10.1016/j.heliyon.2019.e01384

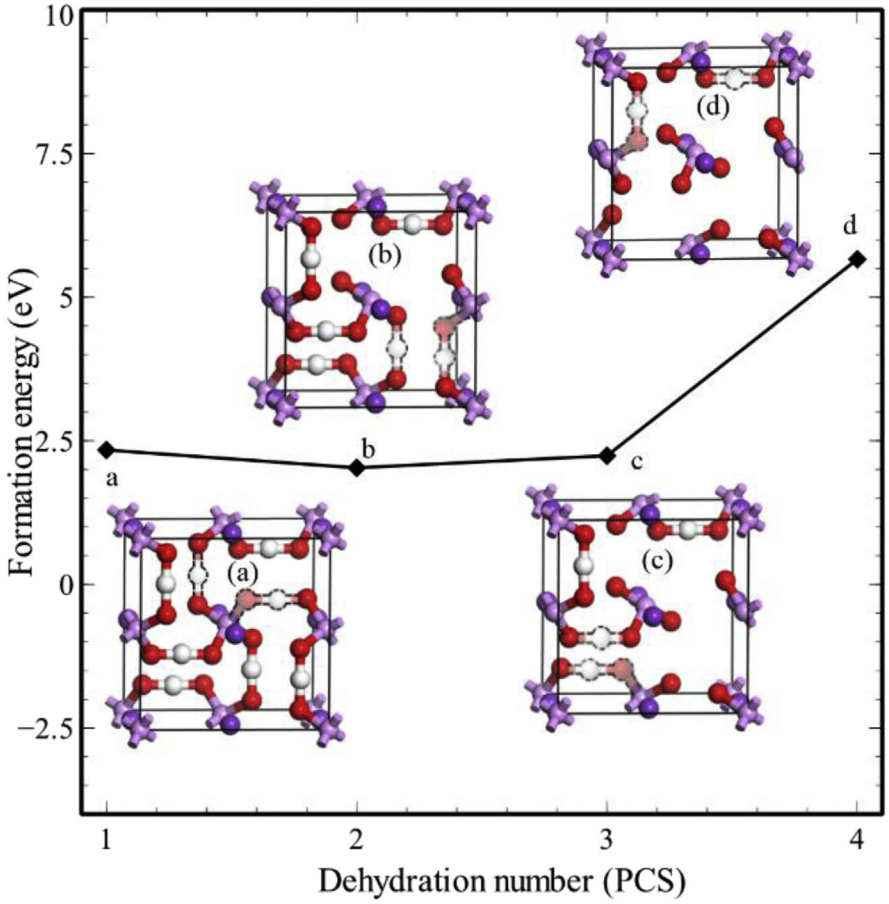

Fig. 2. The formation energy of KDP dehydration process. a. The formation energy of KDP after taking off one water molecule. b. The formation energy of KDP after taking off two water molecules. c. The formation energy of KDP after taking off three water molecules. d. The formation energy of KDP after taking off four water molecules ($(KPO_3)_n$). (a) to (d) are model diagrams corresponding to them, respectively. K is shown in purple, H is shown in white, P is shown in light purple, O is shown in red. The atom in the dotted line indicates the position of the removed water molecule.

product properties after dehydration. During the process of dehydration, the produced water molecules are evaporated. The choice of dehydration sites is random, however for larger models, dehydration starts from the crystal surface, and dehydration becomes more and more difficult as the degree of dehydration deepens [43].

The formation energy of KDP crystal dehydration is shown in Fig. 2. The formation energy during dehydration is positive, indicating that dehydration requires external energy to perform, such as high temperature. As the degree of dehydration deepens, the formation shows a rising trend, which indicates that dehydration will be very difficult [43]. The first three formation energies are all around 2 eV, and the final state of final dehydration, that is, the product becomes $(KPO_3)_n$, and the formation energy is 5.66 eV, indicating that dehydration is relatively easy to implement, however it is difficult to completely dehydrate to form $(KPO_3)_n$.

https://doi.org/10.1016/j.heliyon.2019.e01384

3.2. Electronic properties of dehydration processes

The calculated band gap by GGA-PBE functional in DFT is about 1.3 eV lower than the experimental data of 7.2 eV [2, 3, 4, 5, 39]. While the calculated band gap by HSE functional in DFT is about 7.1 eV, which is closer to the experimental data. Therefore, the density of states (DOS) referred to pure KDP crystal model and four dehydration models of KDP crystal are shown in Fig. 3. Band gaps present a decreasing trend during the dehydration of KDP crystal. By analyzing the partial density of states (PDOS) of every atom in the KDP crystal, the bottom of the conduction band (BCB) of the KDP crystal is mainly contributed by all the K, P and O atoms in the model. By using the same analysis method, the position of the "bottom of the conduction band" corresponding to the following three steps of dehydration should be 7.32, 8.06, and 8.04 eV, respectively, which are mainly contributed by all the K, P and O atoms in the model (Table 1). Therefore, we can determine that these intermediate states are defect states, which are induced by dehydration-process.

In order to analyze the contribution of band structure, we introduce the PDOS of every element to determine the origin of these defective states. In Fig. 3(a), the two main defect states are at 5.04 eV and 6.27 eV, respectively. The former is mainly

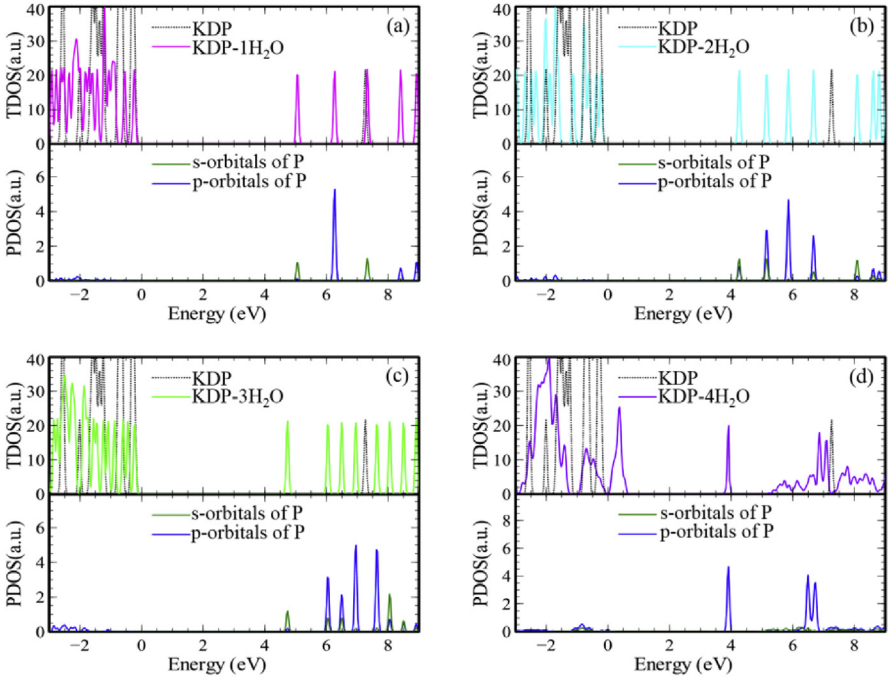

Fig. 3. The TDOS and PDOS of P during the dehydration. (a) The TDOS of KDP after taking off one water molecule is shown in pink. (b) The TDOS of KDP after taking off two water molecules is shown in blue. (c) The TDOS of KDP after taking off three water molecules is shown in green. (d) The TDOS of KDP after taking off four water molecules is shown in purple. The TDOS of KDP is shown in black dotted line. The PDOS of P's s-orbitals is shown in dark green. The PDOS of P's p-orbitals is shown in navy blue.

https://doi.org/10.1016/j.heliyon.2019.e01384

Table 1. The PDOS analysis of unoccupied states near BCB during the thermal dehydration of KDP.

	Unoccupied states near BCB (eV)	Contributed atoms	Unoccupied states near BCB (eV)	Contributed atoms
KDP	7.20	All K, P, O atoms	–	–
KDP-1H_2O	7.32	All K/P atoms, O3, O6 to O10, O12	8.40	All K atoms, O7, O8
KDP-2H_2O	8.06	All K/P atoms, O4 to O6, O8, O9, O11, O14	8.58	O5, O11
KDP-3H_2O	8.04	All K atoms, P1, P3, P4, O2, O4	8.49	K4, P1, P3

contributed mainly by the s-orbitals of the P atoms, and the latter is mainly contributed by the p-orbital of the P atoms. In Fig. 3(b), the p-orbitals of the P atoms mainly contribute to the defect states at 5.13 eV, 5.83 eV and 6.67 eV. The s-orbitals of the P atoms mainly contribute to the defect states at 4.26 eV and 5.13 eV. Similarly, in Fig. 3(c), the s-orbitals of the P atoms mainly contribute to the defect states at 4.70 eV. The p-orbitals of the P atoms mainly contribute to the defect states at 6.02 eV, 6.46 eV and 6.95 eV. Therefore, P atoms in the model contribute a lot to these defect states. In order to explore why the P atoms in the model contribute a lot to the defect states generated during the KDP dehydration process, we calculate differential charge maps of P atoms for analysis.

In Fig. 4, differential charge density calculations are presented. Taking the P atom in the center of the model as an example, we analyzed the changes in its hybridization type during dehydration. When we removed the third water molecule, the H atoms on the O atoms those are connected to the central P atom have all been completely removed. At this time, the PO_3^- structure has formed. In Fig. 4(a), the O-P-O bond angle is 108.9°. In the KDP crystal, P is bonded to the four O atoms around it, of which three are σ bonds and one is π bonds, so it is sp^3 hybridization. In the progress of dehydration, as shown in Fig. 4(b) to Fig. 4(d), the O-P-O bond angle gradually changes to 120°. Fig. 4(d), the central P is gradually in the same plane as its surrounding three O atoms and becomes sp^2 hybridization. At this time, P has one σ bond and two π bonds in the bond connecting the three oxygen atoms around it. We can find that many defect states are formed between 4 eV and 8 eV. These defect states are mainly due to the change of P from sp^3 hybridization to sp^2 hybridization.

In Fig. 3(d), KDP crystal has a defect state at 3.92 eV after removing four waters, which is consistent with experimental data [45]. They used a novel experimental approach to understand the mechanism of laser-induced KDP crystal damage: generating damage thresholds and wavelength maps. Two notable sharp steps centered at 2.55 eV and 3.90 eV are clearly demonstrated in their experimental results. The area between the steps exhibits a smooth reduction in the damage threshold as the wavelength decreases. Liu *et al.* studied the physical properties of H defects in KDP crystals [4]. Their results show that positively charged H vacancies may reduce KDP bandgap value to 2.5 eV, which coincides with the first step of experiment [45].

https://doi.org/10.1016/j.heliyon.2019.e01384

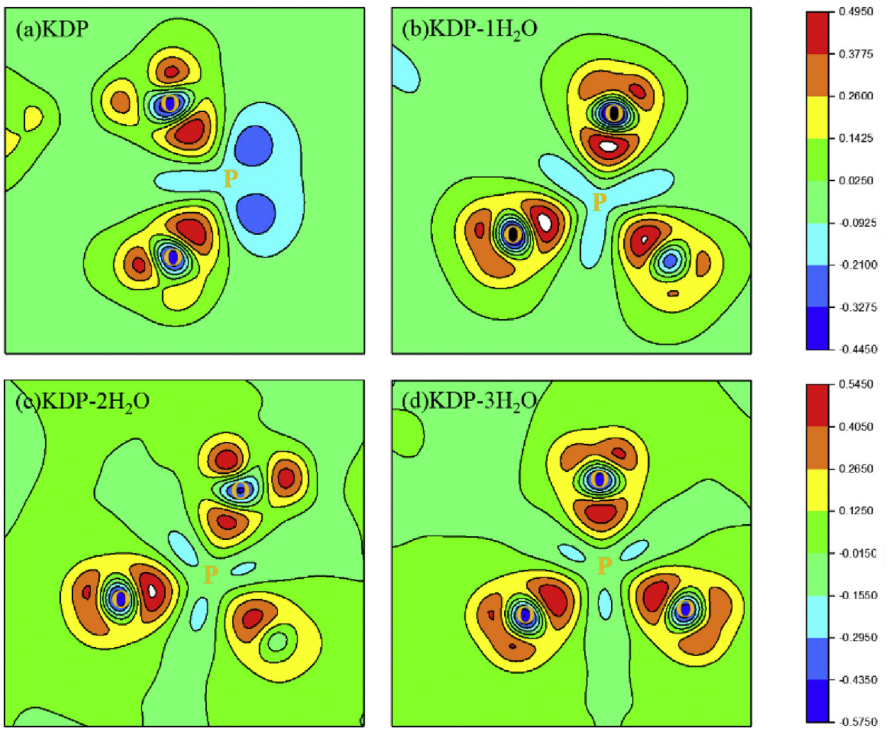

Fig. 4. The differential charge density calculations during the KDP dehydration. (a) The differential charge density of KDP in the O—P—O plane. (b) The differential charge density of KDP after taking off one water molecule in the O—P—O plane. (c) The differential charge density of KDP after taking off two water molecules in the O—P—O plane. (d) The differential charge density of KDP after taking off three water molecules in the O—P—O plane.

Our calculations show that dehydration of KDP crystal may be a source of low damage threshold at 3.9 eV. The defect state at 3.92 eV is also close to 355 nm, which is an important wavelength parameter of KDP triple frequency laser. The nonlinear absorption at 355 nm is identified as two-photon absorption and a nonlinear refraction index with a positive sign indicates the generation of a self-focusing effect in KDP crystal [46]. Liu *et al.* showed that Fe-doped KDP crystal had a defect state at 355 nm [47]. Our results indicate that dehydration may also produce a defect state at 355 nm, which is interesting for the experiment.

3.3. Optical properties of dehydration processes

KDP crystal is an excellent optical material and it is essential for the study of its optical properties. Similarly, we have used the HSE method to calculate the optical absorption spectrum of the dehydration process of KDP crystal. Using the method of the density of states and the optical absorption (DOS and OA) plot comparison analysis, we analyzed the different optical absorption peaks of OA spectra in various stages of dehydration of KDP crystals, which is shown in Fig. 5. From the DOS and OA spectra obtained for each water molecule removed in Fig. 5, it can be seen that as the amount of dehydration increases, the resulting band gap shows a

https://doi.org/10.1016/j.heliyon.2019.e01384

decreasing trend, and the optical absorption in the corresponding optical absorption spectrum also shows a kind of the tendency to move to the infrared region.

Details of some major optical absorption peaks in the OA spectrum are shown in Table 2. We can separate the analysis into two spectral regions: low excitation that go from 5.0 to 7.5 eV and high excitation that lie in the UV region between 8.0 and 9.0 eV. The high excitation seems to exhibit a smaller energy spread than the low excitation. Each high-energy excited single-particle decomposition contains a series of single-particle transitions that involve not only the defect states but also the occupied states from the TVB (Top of Valence Band) domain and the unoccupied states of the BCB (Bottom of Conduction Band) neighborhood. The low energy excitations, which are mainly caused by the transition between occupied and unoccupied defect states, exhibit large energy dispersal due to the large differences in KDP geometry during dehydration. As the final product of dehydration, that is, polymer $(KPO_3)_n$, it exhibits a very wide range of optical absorption, and has its optical absorption peak from the infrared region to the ultraviolet region. Furthermore, the optical absorption characteristics in the near-infrared region are quite high, and particularly high optical absorption peaks appear at 0.35 and 0.87 eV. We can find that OA spectrum tends to have a red-shift with the deepening of dehydration. Low energy excitation exhibits large energy diffusion compared to high energy excitation due to large differences in KDP geometry during dehydration. That is to say,

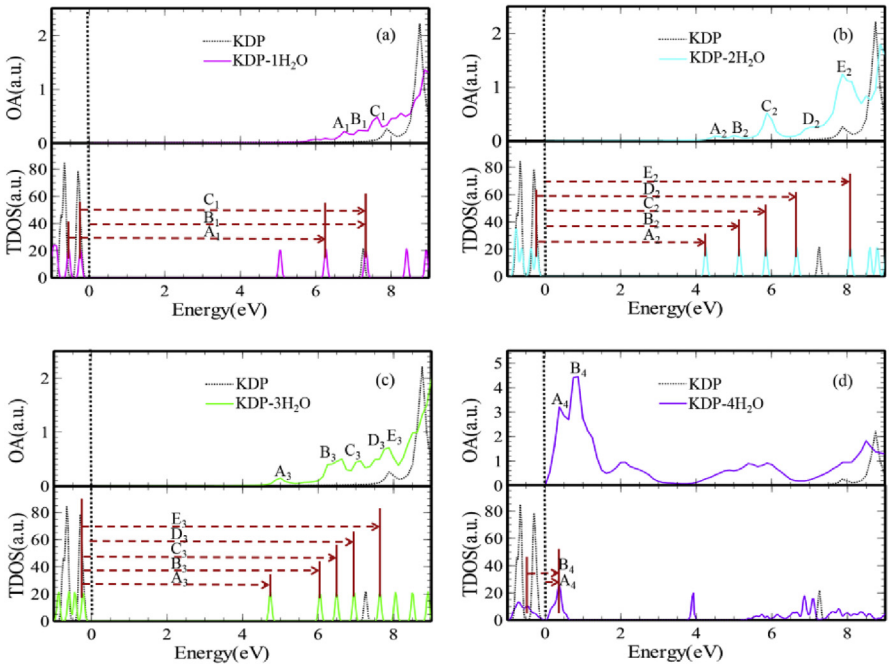

Fig. 5. The density of states and the optical absorption spectrum (DOS and OA) in dehydration of KDP crystals. (a) The DOS and OA of KDP after taking off one water molecule is shown in pink. (b) The DOS and OA of KDP after taking off two water molecules is shown in blue. (c) The DOS and OA of KDP after taking off three water molecules is shown in green. The DOS and OA of KDP after taking off four water molecules is shown in purple. (d) The DOS and OA of KDP are shown in black dotted line.

https://doi.org/10.1016/j.heliyon.2019.e01384

Table 2. Details of the main optical absorption peaks at various stages of dehydration given in Fig. 5. The columns "from/to" provides the details of the positions of the unexcited and excited states that form the corresponding absorption peaks. The notation is the same as that used in Fig. 5.

	Absorption peak	Energy (eV)	From (eV)	To (eV)
KDP-1H_2O	A_1	6.74	−0.57	6.27
	B_1	7.12	TVB	7.32
	C_1	7.62	−0.24	7.32
KDP-2H_2O	A_2	4.50	−0.23	4.26
	B_2	5.01	TVB	5.13
	C_2	5.86	TVB	5.83
	D_2	6.92	−0.23	6.67
	E_2	8.12	TVB	8.06
KDP-3H_2O	A_3	5.01	−0.24	4.70
	B_3	6.25	−0.24	6.02
	C_3	6.61	−0.24	6.46
	D_3	6.98	TVB	6.95
	E_3	7.88	−0.24	7.61
KDP-4H_2O	A_4	0.35	TVB	0.35
	B_4	0.87	−0.48	0.35

the influence of the change in geometry caused by dehydration is more pronounced in the low-energy excitation region. In Fig. 5(d), KDP crystal has an absorption peak at 0.87 eV (B_4) after removing four waters, which is consistent with experimental data 1064 nm (1.1 eV) [48, 49]. 1064 nm is an important parameter in the experiment of KDP crystal. According to our calculations, it can be found that the absorption of KDP crystal at 1064 nm may be caused by KDP dehydration. As shown in Table 2, the optical absorption peak at 0.87 eV (B_4) may be generated by a transition from −0.48 eV to 0.35 eV.

4. Conclusions

In this work, the First-principles method is used to obtain stable structure for the dehydration of 32-atom KDP crystal. The predecessors used the PBE method to calculate the bandgap and some properties of KDP crystal. However, we used the HSE method for the first time to calculate, which is closer to the experimental values. During the dehydration process of KDP, the bandgap value gradually decreases, and an obvious redshift can be observed in the absorption spectrum, resulting in many obvious optical absorption peaks and many defect states in the range of 4 eV to 8 eV. These defect states are mainly due to the change of P atoms from sp^3 hybridization to sp^2 hybridization. Moreover, we find KDP crystal has a defect state at 3.92 eV after removing four waters, which is in good agreement with the experimental values of the C.W. Carr. *et al.* [45]. That indicates dehydration of the KDP crystal may be a source of low damage threshold of 3.9 eV. Our calculations will be interest for the application of KDP crystals in high-temperature laser applications.

https://doi.org/10.1016/j.heliyon.2019.e01384

Declarations

Author contribution statement

Xiang Li: Conceived and designed the experiments; Performed the experiments; Analyzed and interpreted the data; Contributed reagents, materials, analysis tools or data; Wrote the paper.

Pengfei Zhu: Conceived and designed the experiments; Analyzed and interpreted the data; Contributed reagents, materials, analysis tools or data.

Lihong Han: Analyzed and interpreted the data; Wrote the paper.

Tao Zhang: Analyzed and interpreted the data; Contributed reagents, materials, analysis tools or data.

Baonan Jia: Analyzed and interpreted the data; Contributed reagents, materials, analysis tools or data; Wrote the paper.

Shanjun Li, Jun Chen: Conceived and designed the experiments; Contributed reagents, materials, analysis tools or data; Wrote the paper.

Ming Lei: Analyzed and interpreted the data; Wrote the paper.

Pengfei Lu: Conceived and designed the experiments; Analyzed and interpreted the data; Contributed reagents, materials, analysis tools or data; Wrote the paper.

Funding statement

This work was supported by National Natural Science Foundation of China (No. 61675032), National Key Research and Development Program of China (No. 2017YFB0405100), and the Open Program of State Key Laboratory of Functional Materials for Informatics.

Competing interest statement

The authors declare no conflict of interest.

Additional information

No additional information is available for this paper.

Acknowledgements

We acknowledge the computational support from the Beijing Computational Science Research Center (CSRC).

https://doi.org/10.1016/j.heliyon.2019.e01384

References

[1] J. West, Z. Kristallogr, A quantitative X-ray analysis of structure of potassium dihydrogen phosphate (KH_2PO_4), Ferroelectrics 74 (1930) 306−332.

[2] C.S. Liu, C.J. Hou, N. Kioussis, S.G. Demos, H.B. Radousky, Electronic structure calculations of an oxygen vacancy in KH_2PO_4, Phys. Rev. B 72 (2005) 134110 1−5.

[3] C.S. Liu, Q. Zhang, N. Kioussis, Electronic structure calculations of intrinsic and extrinsic hydrogen point defects in KH_2PO_4, Phys. Rev. B 68 (2003) 224107 1−22410711.

[4] C.S. Liu, N. Kioussis, S.G. Demos, H.B. Radousky, Electron- or hole-assisted reactions of H defects in hydrogen-bonded KDP, Phys. Rev. Lett. 91 (1) (2003) 015505 1−4.

[5] K. Wang, C. Fang, J. Zhang, C.S. Liu, R.I. Boughton, S.I. Wang, X.I. Zhao, First-principles study of interstitial oxygen in potassium dihydrogen phosphate crystals, Phys. Rev. B 72 (2005) 184105 1−5.

[6] T.A. Davi, K. Vedam, Pressure dependence of the refractive indices of the tetragonal crystals: ADP, KDP, $CaMoO_4$, $CaWO_4$, and rutile, J. Opt. Soc. Am. 58 (11) (1968) 1446−1451.

[7] G.A. Samara, Pressure dependence of the static and dynamic properties of KH_2PO_4 and related ferroelectric and antiferroelectric crystals, Ferroelectrics 71 (1987) 161−182.

[8] G.A. Samara, Vanishing of the ferroelectric and antiferroelectric states in KH_2PO_2-type crystals at high pressure, Phys. Rev. Lett. 27 (2) (1971) 103−106.

[9] J.J. Deyoreo, Z.U. Rek, N.P. Zaitseva, B.W. Woods, Sources of optical distortion in rapidly grown crystals of KH_2PO_4, J. Cryst. Growth 166 (1996) 291−297.

[10] S.G. Demos, M. Staggs, J.J. Deyoreo, H.B. Radousky, Imaging of laser-induced reactions of individual defect nanoclusters, Opt. Lett. 26 (24) (2001) 1975−1977.

[11] C.W. Carr, H.B. Radousky, M. Staggsa, A.M. Rubenchika, M.D. Feita, S.G. Demosa, Time-resolved spectroscopic investigation of emission observed during damage in the bulk of fused silica and DKDP crystals, Proc. SPIE 4679 (2002) 361−367.

https://doi.org/10.1016/j.heliyon.2019.e01384

[12] A. Surmin, S. Lambert, F. Guillet, B. Minot, D. Damiani, F. Gervais, Thermal mechanism of laser induced damages in KDP crystals, Proc. SPIE 6720 (672007) (2007) 1–5.

[13] L.J. Atherton, F. Rainer, J.J. Deyoreo, I.M. Thomas, N. Zaitseva, F. Demarco, Thermal and laser conditioning of production and rapid-growth KDP and KD*P crystals, SPIE 2114 (1994) 36–45.

[14] B.K. Choi, S.C. Chung, Electrical conductivity and high temperature phase transition studies on KH_2PO_4 crystals, Ferroelectrics 155 (1994) 153–158.

[15] D.M. Fragua, J. Castillo, R. Castillo, R.A. Vargas, New amorphous phase $K_nH_2P_nO_{3n+1}$(n>>1) in KH_2PO_4, Rev. Latin. Am. Metal. Mater. S1 (2) (2009) 491–497.

[16] R.A. Negres, S.O. Kucheyev, P. DeMange, C. Bostedt, T. Van Buuren, A.J. Nelson, S.G. Demos, Decomposition of KH_2PO_4 crystals during laser-induced breakdown, Appl. Phys. Lett. 86 (171107) (2005) 1–5.

[17] K.D. Parikh, D.J. Dave, M.J. Joshi, Crystal growth, thermal, optical, and dielectric properties of L-lydine doped KDP crystals, Mod. Phys. Lett. B 23 (12) (2009) 1589–1602.

[18] K.D. Parikh, D.J. Dave, B.B. Parekh, M.J. Joshi, Growth and characterization of L-alanine doped KDP crystals, Cryst. Res. Technol. 45 (6) (2010) 603–610.

[19] P. Shenoy, K.V. Bangera, G.K. Shivakumar, Growth and thermal studies on pure ADP, KDP and mixed $K_{1-x}(NH_4)_xH_2PO_4$ crystals, Cryst. Res. Technol. 45 (8) (2010) 825–829.

[20] T. Tsujibayashi, M. Ichimiya, K. Toyoda, N. Ohno, Molecular-chain formation induced by infrared-laser light observed in L-cysteine and potassium dihydrogenphosphate, Jpn. J. Appl. Phys. 50 (101601) (2011) 1–4.

[21] C.E. Botez, J.L. Morris, A.J.E. Manriquez, A. Anchondo, Heating induced structural and chemical behavior of KD_2PO_4 in the 25 °C–215 °C temperature range, Mater. Charact. 83 (2013) 74–78.

[22] H. Ettoumi, T. Mhiri, Kinetic process of dehydration at fusion temperature and the high-temperature phase transition in KH_2PO_4, J. Mol. Struct. 1034 (2013) 112–118.

[23] J. Paier, M. Marsman, K. Hummer, G. Kresse, Screened hybrid density functionals applied to solids, J. Chem. Phys. 124 (154709) (2006) 1–13.

[24] J. Heyd, G.E. Scuseria, Assessment and validation of a screened Coulomb hybrid density functional, J. Chem. Phys. 120 (16) (2004) 7274–7280.

https://doi.org/10.1016/j.heliyon.2019.e01384

[25] J. Heyd, G.E. Scuseria, Efficient hybrid density functional calculations in solids: assessment of the Heyd-Scuseria-Ernzerhof screened Coulomb hybrid functional, J. Chem. Phys. 121 (3) (2004) 1187−1192.

[26] J. Heyd, J.E. Peralta, G.E. Scuseria, Energy band gaps and lattice parameters evaluated with the Heyd-Scuseria-Ernzerh of screened hybrid functional, J. Chem. Phys. 123 (174101) (2005) 1−8.

[27] J.E. Peralta, J. Heyd, G.E. Scuseria, Spin-orbit splittings and energy band gaps calculated with the Heyd-Scuseria-Ernzerhof screened hybrid functional, Phys. Rev. B 74 (073101) (2006) 1−4.

[28] L. Wu, P. Lu, R. Quhe, Q. Wang, C. Yang, P. Guan, K. Yang, Stanene nanomeshes as anode materials for Na-ion batteries, J. Mater. Chem. A 6 (17) (2018) 7933−7941.

[29] H. Wang, R. Liu, Y. Li, X. Lu, Q. Wang, S. Zhao, K. Yuan, Z. Cui, X. Li, S. Xin, R. Zhang, M. Lei, Z. Lin, Durable and efficient hollow porous oxide spinel microspheres for oxygen reduction, Joule 2 (2) (2018) 337−348.

[30] Q. Wang, X. Li, L. Wu, P. Lu, Z. Di, Electronic and interface properties in graphene oxide/hydrogen-passivated Ge heterostructure, Phys. Status Solid. RRL 13 (2) (2019), 1800461.

[31] J. Zhang, L. Han, Z. Guan, B. Jia, Z. Peng, X. Guan, B. Yan, G. Peng, P. Lu, Electronic and luminescence characteristics of interstitial Bi^0 atom in bismuth-doped silica optical fiber, J. Lumin. 207 (2019) 346−350.

[32] G. Kresse, J. Hafner, Ab initio molecular dynamics for liquid metals, Phys. Rev. B 47 (1) (1993) 558−561.

[33] G. Kresse, J. Hafner, Ab initio molecular-dynamics simulation of the liquid-metal-amorphous-semiconductor transition in germanium, Phys. Rev. B 49 (20) (1994) 251−269.

[34] K. Itoh, M. Uchimoto, Forty crystal structure analyses of KH_2PO_4 in the para-electric phase, Ferroeleclrics 217 (1998) 155−162.

[35] H. Huang, Z.S. Lin, C.T. Chen, Mechanism of the linear electro-optic effect in potassium dihydrogen phosphate crystals, J. Appl. Phys. 104 (073116) (2008) 1−3.

[36] J.D. Patterson, Density-functional theory of atoms and molecules, Ann. Nucl. Energy 16 (1989) 611−612.

[37] J.P. Perdew, K. Burke, M. Ernzerhof, Generalized gradient approximation made simple, Phys. Rev. Lett. 77 (18) (1996) 3865−3868.

https://doi.org/10.1016/j.heliyon.2019.e01384

[38] Z. Lin, Z. Wang, C. Chen, Mechanism of linear and nonlinear optical effects of KDP and urea crystals, J. Chem. Phys. 118 (5) (2003) 2349−2356.

[39] X. Chen, Q. Zhao, X. Wang, J. Chen, Linear optical properties of defective KDP with oxygen vacancy: first-principles calculations, Chin. Phys. B 24 (7) (2015) 1−6.

[40] H.A.R. Aliabad, M. Fathabadi, I. Ahmad, Optoelectronic properties of KDP by first principle calculations, Int. J. Quantum Chem. 24258 (2012) 1−8.

[41] J. Ding, Y. Zhao, S. Wang, Y. Gu, H. Gui, H. Liu, G. Xu, Investigation on high temperature behavior and thermal dehydration kinetics of KDP crystal, J. Synth. Cryst. 44 (5) (2015) 1227−1232.

[42] J.F. Juradoa, C. Vargas-Hernandez, R.A. Vargas, Raman and structural studies on the high-temperature regime of the KH_2PO_4-$NH_4H_2PO_4$ system, Rev. Mex. Fis. 58 (2012) 411−416.

[43] K. Lee, Hidden nature of the high-temperature phase transitions in crystals of KH_2PO_4-type: is it a physical change? J. Phys. Chem. Solids 57 (3) (1996) 333−342.

[44] E. Ortiz, R.A. Vargas, B.E. Mellander, On the high-temperature phase transitions of some KDP-family compounds: a structural phase transition? A transition to a bulk-high proton conducting phase? Solid State Ionics 125 (1999) 177−185.

[45] C.W. Carr, H.B. Radousky, S.G. Demos, Wavelength dependence of laser-induced damage: determining the damage initiation mechanisms, Phys. Rev. Lett. 91 (12) (2003), 127402:1-4.

[46] D. Cai, Y. Lian, X. Chai, L. Zhang, L. Yang, M. Xu, Effect of anneaxling on nonlinear optical properties of 70% deuterated DKDP crystals at 355 nm, Cryst. Eng. Comm. 20 (2018) 7357−7363.

[47] Y. Liu, X. Li, J. Wu, B. Liu, D. Geng, Y. Zhang, First-principles studies on the electronic and optical properties of Fe-doped potassium dihydrogen phosphate crystal, Comp. Mater. Sci. 143 (2018) 398−402.

[48] S. Pathak, J.A. Dharmadhikari, A. Thamizhavel, D. Mathur, A.K. Dharmadhikari, Growth of micro-crystals in solution by in-situ heating via continuous wave infrared laser light and an absorber, J. Cryst. Growth 433 (2016) 43−47.

[49] Y. Wang, Y. Zhao, X. Peng, G. Hu, M. Zhu, J. Shao, Influence of the size and concentration of precursor on laser damage performance in KDP crystal, Proc. SPIE 10014 (2016), 100141T:1-4.

https://doi.org/10.1016/j.heliyon.2019.e01384